ACTA SCIENTIARUM POLONORUM

Acta Sci. Pol. Technol. Aliment. 25(3) 2026, 297–308

www.food.actapol.net pISSN 1644-0730 eISSN 1898-9594 http://doi.org/10.17306/J.AFS.001505

ORIGINAL PAPER

Received: 29.01.2026
Accepted: 05.05.2026

MICROENCAPSULATION OF IRON AND ZINC USING WHEY PROTEIN ISOLATE AND MALTODEXTRIN WALL SYSTEMS FOR MILK POWDER FORTIFICATION

Vania Zulfa Adristy, Dyah Hesti Wardhani, Siswo Sumardiono, Noer Abyor Handayani✉

Department of Chemical Engineering, Faculty of Engineering, Universitas Diponegoro
Tembalang, Semarang, Central Java 50275, **Indonesia**

ABSTRACT

Background. Iron and zinc are essential micronutrients frequently deficient in the human diet; however, their direct incorporation into food systems can cause instability, oxidation, and reduced bioavailability. This study examined the effects of wall material composition and fortificant ratio on the microencapsulation, release behaviour, and bioavailability of iron and zinc, with a view to application in milk powder fortification.
Material and methods. Microparticles were produced by spray drying across varying ratios of whey protein isolate (WPI) to maltodextrin (7:0, 5:2, 1:1, 2:5, 0:7) and iron to zinc (1:1, 2:1, 1:2).
Results. The highest encapsulation efficiencies were achieved at a 1:1 ratio of both WPI:maltodextrin and iron:zinc, reaching 84.31% for iron and 90.79% for zinc. Zinc demonstrated higher bioavailability than iron, attributable to differences in release behaviour and solubility. Release kinetics confirmed this distinction, with zinc following a first-order model and iron following a Weibull model. When incorporated into milk powder, the microparticles conferred improved mineral bioavailability to the fortified product.
Conclusion. This study highlights the potential of WPI and maltodextrin as wall materials for improving micronutrient delivery in fortified dairy products, providing a basis for subsequent investigations into functional food matrix strategies aimed at enhancing iron and zinc bioavailability.

Keyword: micronutrient deficiency, microencapsulation, iron, zinc, fortification

INTRODUCTION

Deficiencies in essential minerals such as iron and zinc represent a major challenge in developing and underdeveloped countries (Blanco-Rojo and Vaquero, 2019). Iron deficiency is the leading cause of anaemia, driven by low iron intake, the presence of antinutrients that inhibit absorption, and deficiencies in vitamins A, E, B12, and folate (Kumar et al., 2024; Qiu et al., 2025). According to WHO (2021), anaemia affects approximately 29.9% of all women of reproductive age (15–49 years) globally, with higher prevalence among pregnant women in the same age group (36.5%) and children under five (39.8%) (Gupta et al., 2023). Zinc deficiency affects approximately 17% of the global population, equivalent to around 1.1 billion people, and can impair the nervous, digestive, immune and skeletal systems, while also reducing immunity and stunting growth (Zhang et al., 2022).

Fortification is a safe, cost-effective, and sustainable strategy for preventing micronutrient deficiencies through the addition of vitamins and minerals to food

✉noer.abyor@che.undip.ac.id; https://orcid.org/0000-0001-7962-1544

(Olson et al., 2021). However, fortification of iron and zinc in particular faces considerable obstacles, including chemical reactions such as redox reactions and the formation of iron-polyphenol complexes. These reactions can alter the sensory properties, including taste, texture and colour, thereby reducing consumer acceptance (Pratap-Singh and Leiva, 2021). Microencapsulation offers an effective approach to address these challenges by encapsulating iron and zinc to protect them from external influences, improving stability, minimising nutrient loss, masking undesirable tastes and odours, enabling controlled release, and preventing adverse interactions within food systems (Baldelli et al., 2022; Li et al., 2022; Kaul et al., 2022).

The selection of appropriate wall materials is critical for storage stability, encapsulation efficiency, and resistance to gastric and intestinal conditions (Calderón-Oliver and Ponce-Alquicira, 2022). Maltodextrin is a polysaccharide widely used in the food industry for its capacity to function as a matrix-forming and water-binding agent; however, its low surface activity limits the formation of a strong protective layer on droplet surfaces. Proteins, by contrast, serve as effective emulsifiers owing to their amphiphilic nature, ability to reduce interfacial tension, and capacity to form stable protective films around droplets (Lekshmi et al., 2021). Recent studies have explored whey protein isolate (WPI) in microencapsulation systems; WPI readily interacts with carbohydrates to form stable microcapsule structures and functions as a protein with physicochemical properties that support the formation of biopolymer molecular networks (Poopan et al., 2024). Spray drying is a widely used microencapsulation technique suitable for protecting a wide range of materials, including minerals, across diverse wall material systems. It is extensively employed in the food industry for its cost-effectiveness, rapid processing, operational flexibility, and suitability for continuous, large-scale production (Busto et al., 2022).

Although numerous studies have investigated iron and zinc fortification in food systems, research employing microencapsulation with varied ingredient combinations to simultaneously fortify both minerals remains limited. In this study, iron and zinc were microencapsulated by spray drying with varying ratios of WPI and maltodextrin as wall materials and varying ratios of iron to zinc, with a view to application in fortified milk powder. The microcapsules were characterised for encapsulation efficiency and physicochemical properties, while release behaviour, release kinetics, and in vitro bioavailability of iron and zinc under simulated gastric and intestinal conditions were evaluated to elucidate mineral release from the WPI–maltodextrin matrix. These evaluations were conducted to support the development of fortified milk powder products with acceptable physicochemical properties.

MATERIALS AND METHODS

Materials

Iron ($FeSO_4 \cdot 7H_2O$), zinc ($ZnSO_4 \cdot 7H_2O$), hydrochloric acid (37%), 1,10-phenanthroline monohydrate (GR, ACS grade), and buffer solution were obtained from Merck KGaA (Darmstadt, Germany). Maltodextrin was supplied by Lihua (China), and WPI was sourced from Puro Pure Nutrition (Sukoharjo, Indonesia). Nitric acid (70%) and hydroxylamine hydrochloride were purchased from Loba Chemie (Mumbai, India). Acetic acid was supplied by CV Indrasari (Semarang, Indonesia). All chemicals were of analytical grade.

Preparation of microparticles

A feed solution was prepared by dissolving WPI, maltodextrin, $FeSO_4 \cdot 7H_2O$, and $ZnSO_4 \cdot 7H_2O$ in distilled water to a total volume of 300 mL and stirring with a magnetic stirrer until fully hydrated. For the wall material variation, iron and zinc were added at a fixed ratio of 1:1, each at a concentration of 1.5% (w/v), while the WPI:maltodextrin ratio was varied at 7:0, 5:2, 1:1, 2:5, and 0:7 (w/v). For the fortificant ratio variation, the WPI:maltodextrin ratio was fixed at 1:1, each at 3.5% (w/v), and the Fe:Zn ratio was adjusted to 1:1, 2:1, and 1:2. The total solid content in each formulation was 10% (w/v). The suspensions were homogenised at 1,200 rpm for 7 min and spray dried at an inlet temperature of 160°C and an outlet temperature of 80°C (Mini Buchi B-290), with an inlet temperature of 160°C and an outlet temperature of 80°C (Mini Buchi B-290), a feed flow rate of 5 mL/min, and a vacuum pressure of 90%.

Determination of encapsulation efficiency (EE) and mineral loading

For iron, 20 mg of microparticles were dissolved in 25 mL of 2.5% (v/v) acetic acid and 0.5 mL of 37%

HCl, following a modified procedure described by Handayani et al. (2023). The solution was heated to 80°C and stirred at 250 rpm for 2 h, then cooled and filtered through Whatman No. 1 filter paper. Subsequently, 2 mL of the filtrate was combined with 0.6 mL of hydroxylamine hydrochloride and left in the dark for 5 min. Thereafter, 1 mL of acetate buffer, 0.6 mL of 1,10-phenanthroline, and 0.8 mL of distilled water were added. Absorbance was measured at 510 nm using a UV-Vis spectrophotometer. A calibration curve was prepared using standard iron solutions at concentrations of 0.5–5 mg/L following the same procedure.

For zinc, 20 mg of microparticles were added to 10 ml of 70% HNO_3 and digested in an incubator shaker for 24 h at 50°C and 200 rpm, following a modified method of Pratap-Singh and Leiva (2021). An aliquot of 1 mL was then diluted with distilled water to 25 mL, and zinc content was determined by atomic absorption spectrophotometry (AAS). Encapsulation efficiency and mineral loading were calculated using the following equations.

$$\%EE = \frac{\text{Total weight of iron/zinc in the microparticles}}{\text{Total weight of iron/zinc used}} \times 100\% \quad (1)$$

$$\text{Iron Loading} = \frac{\text{Total weight of iron in the microparticles}}{\text{100 mg microparticles}} \quad (2)$$

$$\text{Zinc Loading} = \frac{\text{Total weight of zinc in the microparticles}}{\text{100 mg microparticles}} \quad (3)$$

SEM and FTIR analysis

The surface morphology and structural features of the microparticles were examined by scanning electron microscopy (SEM). Fourier transform infrared (FTIR) spectroscopy was employed to identify functional groups and assess potential molecular interactions between iron, zinc, and the wall materials within the microencapsulated system.

Particle size analysis

The surface morphology of the microparticles was examined using a scanning electron microscope (SEM), and representative micrographs were used to illustrate the results. Average particle size was determined by measuring 30 individual microparticles per sample, restricted to particles within the same focal plane to minimise perspective errors and ensure measurement consistency. Particle size was subsequently analysed using ImageJ and OriginLab software.

Colour analysis

Iron and zinc microparticles were photographed against a white background. Colour was assessed using the Hunter colour system (L*, a*, and b*), and ΔE values for selected samples were calculated using a colourimeter.

In vitro iron and zinc release kinetics

A modified method based on Handayani et al. (2023) was used. Iron/zinc microparticles (20 mg) were placed in a micromesh tea bag and immersed in 100 mL of simulated gastric fluid (SGF, pH 1.2) for 2 h at 37°C. Subsequently, 100 mL of simulated intestinal fluid (SIF, pH 6.8) was added and digestion continued for a further 4 h. Aliquots of 10 mL were collected at 30, 60, 120, 180, 240, 360, and 480 min, with an equal volume of fresh SGF or SIF replaced after each collection. Released iron was analysed by UV–Vis spectrophotometry at 510 nm, while zinc was determined by AAS. The release profiles were subsequently fitted to five commonly applied mathematical models – zero-order, first-order, Hixson–Crowell, Weibull, and Higuchi – using regression analysis. The model yielding a coefficient of determination (R^2) closest to unity (1.0) was considered the best fit.

In vitro iron and zinc bioavailability

Iron/zinc microparticles (20 mg) were placed in a tea bag and immersed in 25 mL of SGF, then incubated in a shaker incubator at 37°C for 1 h. Subsequently, 25 mL of SIF was added, and incubation continued for a further 3 h. Released iron was quantified by UV–Vis spectrophotometry at 510 nm, and zinc was quantified by AAS. Bioavailability was calculated using the following equations.

$$\text{Iron bioavailability} = \frac{\text{Iron content in the digestive fluid}}{\text{Total iron content in the microparticles}} \quad (4)$$

$$\text{Zinc bioavailability} = \frac{\text{Zinc content in the digestive fluid}}{\text{Total zinc content in the microparticles}} \quad (5)$$

Iron and zinc fortification of milk powder

Fortification of powdered cow's milk was carried out by dry blending, incorporating 200 mg of iron and zinc microparticles into a single serving of milk powder (30 g). The bioavailability of iron and zinc was assessed alongside a qualitative assessment of macroscopic physical attributes – such as colour, texture, and odour – to evaluate the overall visual and sensory consistency of the fortified product.

Statistical analysis

Data were analysed using one-way ANOVA followed by Tukey's HSD post-hoc test at a significance level of $p \leq 0.05$. All analyses were performed in triplicate, and results are expressed as mean ± standard deviation.

RESULTS AND DISCUSSION

Encapsulation efficiency and mineral loading of iron and zinc microparticles

In formulations prepared with varying WPI:maltodextrin ratios, the encapsulation efficiency of iron ranged from 80.43–84.31%, while zinc exhibited slightly higher efficiencies of 89.89–90.79%, as shown in Figure 1(a). Figure 1(b) shows that the loading of iron and zinc within the microparticles was 2.573–2.698 mg and 2.876–2.905 mg per 100 mg of microparticles, respectively. These results indicate a slightly lower encapsulation efficiency for iron but a markedly higher value for zinc compared with those reported in previous studies (Singh and Prasad, 2023). Both minerals nevertheless exhibited greater loading values, which may be attributable to the formation of a more compact encapsulation matrix that improved mineral retention during spray drying. The combination of WPI and maltodextrin demonstrated superior encapsulation performance and mineral loading relative to the use of either individual wall material alone, and appeared to promote the formation of a more stable and uniform encapsulation matrix (Poopan et al., 2024).

The encapsulation efficiency of the microparticles varied with the iron:zinc ratio, as shown in Figure 2(a), ranging from 68.13–91.28% for iron and 66.98–90.79% for zinc. At the balanced ratio (1:1), both minerals showed relatively stable efficiencies, whereas under iron-rich (2:1) and zinc-rich (1:2) conditions, the dominant mineral tended to show lower efficiency, potentially attributable to the mineral content exceeding the encapsulation capacity of the matrix. As presented in Figure 2(b), iron content ranged from 1.988–2.848 mg and zinc content from 1.620–2.905 mg per 100 mg of microparticles. The highest iron loading was observed at the 2:1 ratio, while the highest zinc loading was found at the 1:2 ratio. A similar trend was reported by Kaul et al. (2022), in which increased

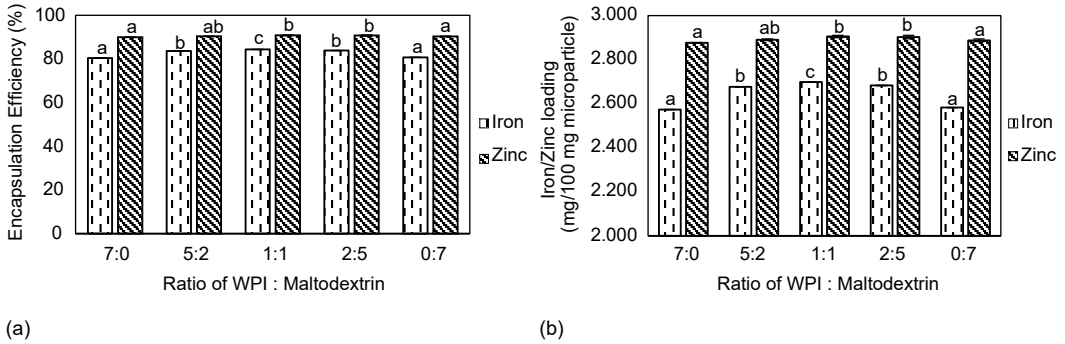

Fig. 1. Encapsulation efficiency (a) and mineral loading (b) of iron and zinc microparticles at varying WPI:maltodextrin ratios

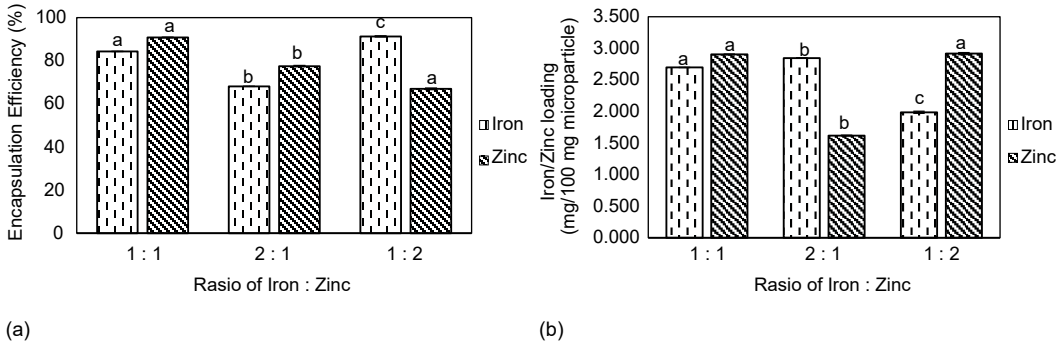

Fig. 2. Encapsulation efficiency (a) and mineral loading (b) of iron and zinc microparticles at varying iron:zinc ratios

iron or zinc content resulted in higher mineral retention within the encapsulated matrix.

Morphological characterisation

SEM analysis of the iron and zinc microparticles revealed distinct morphological characteristics across samples of varying compositions. As shown in Figure 3(a), microparticles produced with WPI alone exhibited irregular shapes and wrinkled surfaces with central voids, whereas those produced with maltodextrin alone, Figure 3(b), displayed smoother surface structures but also presented central cavities. Such surface irregularities and cavities can render bioactive components more susceptible to oxidation due to reduced protection, thereby decreasing encapsulation efficiency (Sirichokworrakit et al., 2025). The combination of WPI and maltodextrin, Figure 3(c), produced microparticles with a more spherical morphology, smoother surfaces, and fewer surface irregularities compared with those formed using either wall

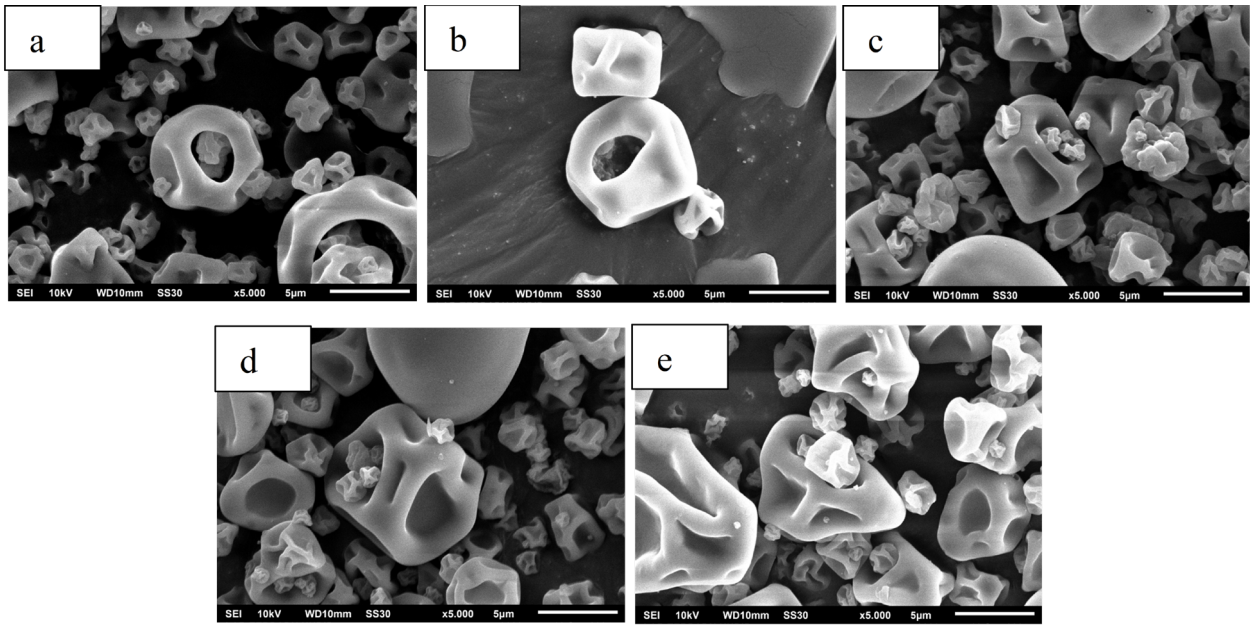

Fig. 3. Surface morphology of iron and zinc microparticles produced with varying WPI:maltodextrin ratios [(a) 7:0, (b) 0:7, and (c) 1:1] and iron:zinc ratios [(d) 2:1 and (e) 1:2]

alone. The incorporation of maltodextrin contributed to improved film formation during drying, resulting in a more uniform and stable microparticle structure (Kaul et al., 2022), while WPI produced a more cohesive wall matrix through protein denaturation, leading to the formation of a tightly interconnected molecular network (Sirichokworrakit et al., 2025).

Variations in the iron:zinc ratio also influenced microparticle morphology. At the 1:1 ratio, Figure 3(c), particles appeared spherical with slightly wrinkled surfaces. At the 2:1 ratio, Figure 3(d), the particles exhibited rougher surfaces, whereas at the 1:2 ratio in Figure 3(e), they appeared more porous and irregular in shape. The surface wrinkles and indentations observed across samples may also be attributed to the rapid evaporation of water during spray drying, which promotes the formation of a crust layer on the droplet surface at the early stage of drying (Ledari et al., 2024).

Functional group characterisation

The FTIR spectra of WPI, maltodextrin, and iron and zinc microparticles prepared at a 1:1 WPI:maltodextrin ratio and 1:1 iron:zinc ratio were recorded across the range of 4,000–500 cm^{-1}, as shown in Figure 4. Strong absorption bands at 3,273 and 2,932 cm^{-1} correspond to the stretching vibrations of hydroxyl (–OH) and methyl (–CH) groups, characteristic of maltodextrin (Kaul et al., 2022). An absorption band at 1025 cm^{-1}, associated with the ether (C–O–C) linkage commonly found in polysaccharides, is also attributable to maltodextrin. The characteristic peaks of WPI appear at 1,636 cm^{-1} corresponding to C=O bond stretching of amide I; 1,537 cm^{-1} arising from a combination of C–N bond stretching and N–H bending of amide II; and 1,443 cm^{-1} attributed to N–H in-plane deformation of amide III (Lekshmi et al., 2021). An absorption peak at 1,078 cm^{-1} indicates the presence of sulphate groups, while C–C vibrations and C–S stretching are observed at 1,025 cm^{-1} and 604 cm^{-1}, respectively (Kaul et al., 2022). The retention of functional groups characteristic of both the core and wall materials in the FTIR spectra indicates that these components were preserved within the system following encapsulation, and that the process did not cause significant alterations to the chemical structure of either material.

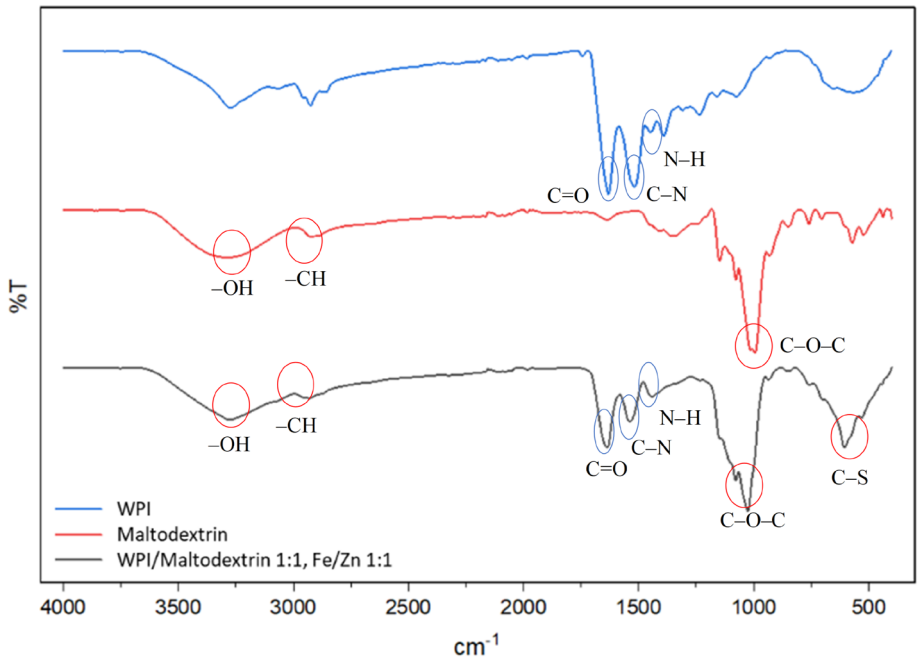

Fig. 4. FTIR spectra of WPI, maltodextrin, and iron and zinc microparticles prepared at a 1:1 WPI:maltodextrin ratio and a 1:1 Fe:Zn ratio

Particle size distribution

Microparticles prepared with a WPI:maltodextrin ratio of 7:0 exhibited the largest average particle size, whereas the smallest was observed at a ratio of 0:7. Microparticles prepared at the 1:1 WPI:maltodextrin ratio produced consistent intermediate sizes across all iron:zinc ratios. This may be attributed to the tendency of whey proteins to undergo denaturation and aggregation during spray drying, which increases the viscosity of the feed solution, promoting the formation of larger droplets and consequently larger microparticles (Sirichokworrakit et al., 2025).

Table 1. Particle size distribution of iron and zinc microparticles at varying wall material and fortificant ratios

WPI:Maltodextrin	Iron:Zinc	Particle size, µm
7:0	1:1	1.645 ±0.06305[a]
1:1	1:1	1.577 ±0.08893[b]
0:7	1:1	1.357 ±0.08893[c]
1:1	2:1	1.533 ±0.08509[b]
1:1	1:2	1.524 ±0.08893[b]

Colour

As shown in Table 2, samples with higher maltodextrin proportions appeared lighter and closer to the control, while higher WPI content produced darker microparticles with more pronounced colour differences. Regarding the iron:zinc ratio, the 1:2 formulation appeared brighter than the 2:1 formulation, indicating that a higher proportion of zinc contributed to lighter microparticles, whereas iron tended to produce a darker appearance.

In vitro release profile and kinetic modelling of iron and zinc microparticles

The release profile of iron and zinc microparticles prepared at a 1:1 WPI:maltodextrin ratio is presented in Figure 5. Both minerals exhibited relatively rapid release during the first two hours in simulated gastric fluid (SGF), with release rates of 71% for iron and 47% for zinc. The binary WPI-maltodextrin matrix slowed the release of both minerals compared with earlier studies, indicating that wall material composition influences release behaviour. Release continued to increase during the subsequent four hours in simulated intestinal fluid (SIF), reaching 82% for iron and 92% for zinc. This gradual release pattern indicates that the majority of mineral content was released progressively under simulated gastrointestinal conditions. Under physiological conditions, the released iron and zinc would remain in a bioavailable form available for intestinal absorption (Pratap-Singh and Leiva, 2021).

The release profiles of iron and zinc from WPI–maltodextrin microparticles exhibited distinct release mechanisms, as evidenced by the kinetic model fitting presented in Figure 6. Iron release was best described by the Weibull model, which returned the highest coefficient of determination (R^2) among all models tested. The Weibull model is an empirical approach widely used to characterise release kinetics from heterogeneous matrix systems, owing to its flexibility in representing diverse release patterns. Zinc release was best

Table 2. Colour parameters of iron and zinc microparticles at varying wall material and fortificant ratios

WPI:Maltodextrin	Iron:Zinc	L*	a*	b*	ΔL*	ΔE*
7:0	1:1	69.33 ±13.42	5.33 ±3.21	39 ±7.93	–29.67	47.08
5:2	1:1	77.67 ±9.6	1.67 ±1.15	35.67 ±2.51	–21.33	39.11
1:1	1:1	79.33 ±11.23	1.33 ±2.31	23.00 ±2.64	–19.67	28.15
2:5	1:1	79.67 ±6.65	1.33 ±2.08	30.67 ±2.51	–19.33	33.83
0:7	1:1	94.00 ±7.81	–1.67 ±0.5	3.67 ±1.15	–5.00	5.09
1:1	2:1	75.33 ±10.26	3.67 ±1.53	32.67 ±1.53	–23.67	38.24
1:1	1:2	85.00 ±4.58	2.67 ±1.15	31 ±1	–14.00	31.52

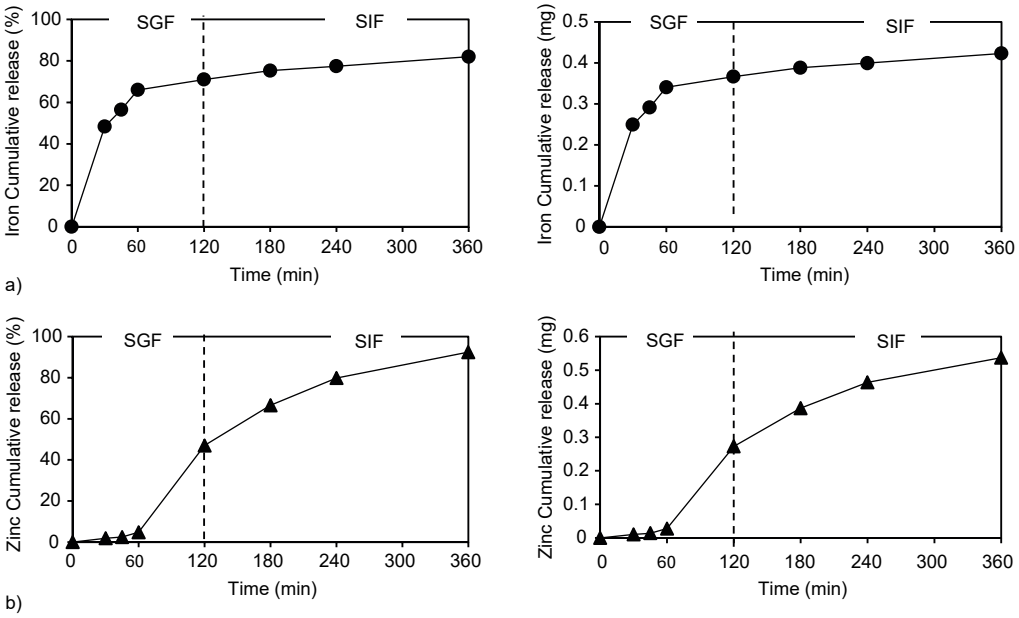

Fig. 5. Cumulative release (percentage and absolute) profiles of iron (a) and zinc (b) from WPI–maltodextrin (1:1) microparticles under simulated gastrointestinal conditions

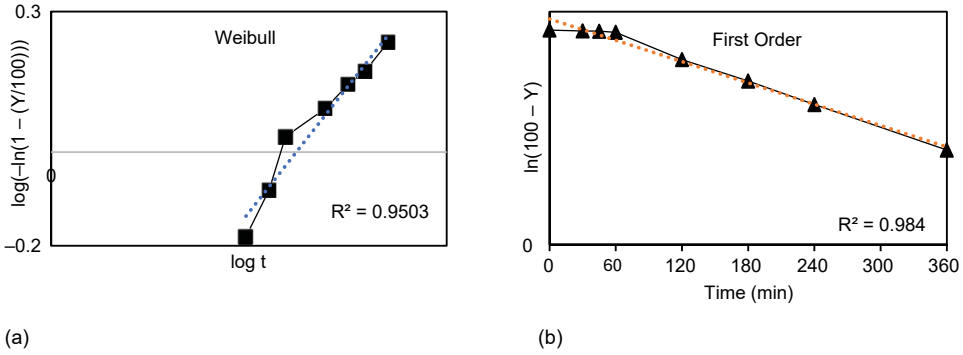

Fig. 6. Iron release kinetics modelled using the Weibull equation (a), and zinc release kinetics following the first-order model (b)

described by the first-order kinetic model, in which the release rate is proportional to the amount of zinc remaining within the microparticles. This suggests that zinc release is governed by the concentration gradient between the WPI-maltodextrin matrix and the release medium, resulting in a progressively decreasing release rate as mineral content within the particles is depleted (Heredia et al., 2022).

In vitro iron and zinc bioavailability

The bioavailability of iron in the iron and zinc microparticles ranged from 8.50–8.91%, while zinc ranged from 15.14–16.23%, as shown in Figure 7(a). The highest bioavailability values for both minerals were achieved with the combination of WPI–maltodextrin wall material compared with either material alone. The binary system formed by combining both materials enhances microparticle stability and protects the minerals during digestion, resulting in more controlled release in the intestine (Figueiredo et al., 2025).

For the fortificant ratio variation, iron bioavailability ranged from 8.23–10.04%, and zinc from 15.14–21.60%, as shown in Figure 7(b). These values are consistent with physiological absorption capabilities:

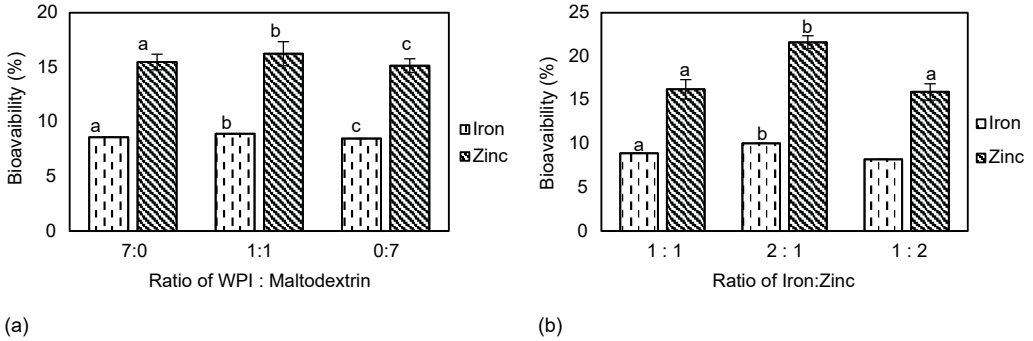

Fig. 7. Bioavailability of iron and zinc from microparticles prepared with varying WPI:maltodextrin ratios (a) and iron:zinc (b)

zinc absorption from food typically ranges from 16–50% (Ośko et al., 2023), whereas non-haem iron absorption is considerably lower, at approximately 2–20%, and is highly influenced by other dietary components consumed simultaneously (Qin et al., 2025). Although variations in WPI:maltodextrin and iron:zinc ratio produced different bioavailability values, zinc consistently showed approximately twice the bioavailability of iron across all formulations. This difference is attributable to their distinct release mechanisms during digestion: zinc, following first-order kinetics, was released more rapidly, allowing greater intestinal absorption, whereas iron, following the Weibull model, exhibited a slower and more complex release pattern. The higher bioavailability of zinc may also be related to its capacity to form soluble complexes with amino acids such as methionine and histidine, while iron tends to oxidise and form insoluble complexes that limit absorption (Ohanenye et al., 2021).

Bioavailability and physical characteristics of iron and zinc-fortified milk powder

The 1:1 WPI:maltodextrin and iron:zinc ratio was selected as the optimal formulation, as it provided the highest mineral loading for both minerals. Based on the mineral content, the addition of 200 mg of the microparticles to 30 g of milk powder is estimated to supply approximately 67% of the daily iron requirement and 73% of the daily zinc requirement for children aged 9–13 years. However, the actual contribution would depend on bioavailability under physiological conditions. Figure 8 presents the bioavailability of iron and zinc in the microparticles and fortified milk powder.

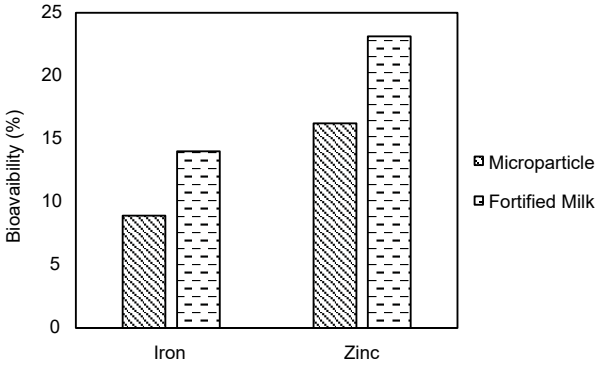

Fig. 8. Bioavailability of iron and zinc in microparticles and fortified milk powder

The fortified milk powder exhibited higher bioavailability values, reaching 14% for iron and 21.13% for zinc. The improved bioavailability in the food matrix may be attributed to interactions between mineral ions and milk proteins, particularly casein and whey proteins, which are naturally present in milk powder (Subroto et al., 2023). In addition, peptides generated during protein hydrolysis, together with sulfur-containing amino acids such as cysteine, contribute to enhanced mineral bioaccessibility by converting ferric iron to the more readily absorbed ferrous form (Shilpashree et al., 2020).

Qualitative assessment showed that the fortified milk powder exhibited no perceptible differences in texture or odour compared with the control. As shown in Figure 9, both samples displayed a uniform macroscopic appearance and maintained the typical characteristics of milk powder, with no noticeable

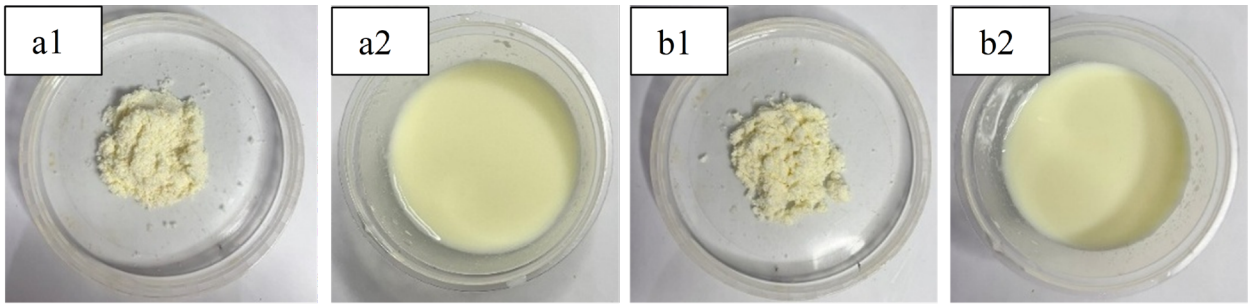

Fig. 9. Visual appearance of control milk powder (a1: powder form; a2: reconstituted form) and iron-zinc fortified milk powder (b1: powder form; b2: reconstituted form)

Table 3. Colour parameters of control and fortified milk powder in powder and reconstituted forms.

Sample	L*	a*	b*
Milk powder (control)	86.67 ±1.15	–5.00 ±0.00	23.67 ±4.04
Fortified milk powder	90.00 ±0.00	–5.00 ±0.00	16.33 ±1.52
Reconstituted milk (control)	85.00 ±1.00	–7.33 ±0.00	24.00 ±0.00
Reconstituted fortified milk	85.00 ±1.73	–8.00 ±1.15	27.00 ±0.00

metallic odour. Colour analysis, presented in Table 3, demonstrated that lightness (L*) and redness (a*) remained stable across both the powder and reconstituted forms, with high L* values and a constant a* value of −5.00. Although fortification caused a slight decrease in yellowness (b*) in the powder form and a minor increase upon reconstitution, these differences were visually imperceptible, preserving the uniform appearance of the product. These findings suggest that the microencapsulation process effectively masked the inherent metallic characteristics of the iron and zinc fortificants, and the incorporation of the microparticles successfully maintained the macroscopic appearance and aroma profile of the fortified milk powder.

CONCLUSION

This study developed WPI–maltodextrin microparticles containing iron and zinc via spray drying and evaluated their application in milk powder fortification. The 1:1 WPI:maltodextrin formulation produced stable, spherical microparticles with the highest encapsulation efficiency and controlled mineral release. Iron release followed the Weibull model, whereas zinc followed first-order kinetics; zinc consistently demonstrated higher bioavailability than iron across all formulations. The fortified milk powder exhibited no perceptible differences in colour, texture, or odour compared with the control, indicating that microencapsulation effectively preserved product quality. These findings confirm that WPI–maltodextrin microencapsulation represents a viable strategy for improving mineral stability and bioavailability in milk-based fortification systems.

ACKNOWLEDGMENTS

This study was financially supported by Universitas Diponegoro through the “RAR” scheme under contract number 222-078/UN7.D2/PP/IV/2025.

DECLARATIONS

Data statement

All data supporting this study has been included in this manuscript.

Ethical approval
Not applicable.

Competing interests
The authors declare that they have no conflicts of interest.

OPEN ACCESS

REFERENCES

Baldelli, A., Liang, D.Y., Guo, Y., Pratap-Singh, A. (2022). Effect of the formulation on mucoadhesive spray-dried microparticles containing iron for food fortification. Food Hydrocolloids, 134, 107906. https://doi.org/10.1016/j.foodhyd.2022.107906

Blanco-Rojo, R., Vaquero, M.P. (2019). Iron bioavailability from food fortification to precision nutrition. A review. Innov. Food Sci. Emerg. Technol., 51, 126–138. https://doi.org/10.1016/j.ifset.2018.04.015

Busto, M.D., González-Temiño, Y., Albillos, S.M., Ramos-Gómez, S., Pilar-Izquierdo, M.C., Palacios, D., Ortega, N. (2022). Microencapsulation of a commercial food-grade protease by spray drying in cross-linked chitosan particles. Foods, 11(14), 2077. https://doi.org/10.3390/foods11142077

Calderón-Oliver, M., Ponce-Alquicira, E. (2022). The role of microencapsulation in food application. Molecules, 27(5), 1499. https://doi.org/10.3390/molecules27051499

Figueiredo, M., Sárkány, Z., Rocha, F. (2025). Challenges and advances in the encapsulation of bioactive ingredients using whey proteins. Foods, 14(4), 691. https://doi.org/10.3390/foods14040691

Gupta, B.B., Mishra, S.K., Banoth, S.K., Baliyan, S., Chauhan, H. (2023). Iron and zinc biofortification of rice by synergistic expression of OsNAS2 gene with monocot (*Pennisetum glaucum*) and dicot (*Phaseolus vulgaris*) ferritins. Plant Physiol. Biochem., 205, 108195. https://doi.org/10.1016/j.plaphy.2023.108195

Handayani, N.A., Mulia, K., Kartohardjono, S., Krisanti, E.A. (2023). Fortifying jelly foods with microencapsulated anti-anaemic compounds, ferrous gluconate, ascorbic acid and folic acid. J. Food Sci. Technol., 60(1), 147–159. https://doi.org/10.1007/s13197-022-05599-7

Heredia, N.S., Vizuete, K., Flores-Calero, M., Pazmiño K.V., Pilaquinga, F., Kumar, B., Debut, A. (2022). Comparative statistical analysis of the release kinetics models for nanoprecipitated drug delivery systems based on poly (lactic-co-glycolic acid). PLOS ONE, 17(3), e0264825. https://doi.org/10.1371/journal.pone.0264825

Kaul, S., Kaur, K., Mehta, N., Dhaliwal, S.S., Kennedy, J.F. (2022). Characterization and optimization of spray dried iron and zinc nanoencapsules based on potato starch and maltodextrin. Carbohydr. Polym., 282, 119107. https://doi.org/10.1016/j.carbpol.2022.119107

Kumar, A.M.S., Ray, A., Sakhare, S.D. (2024). Pre and post milling fortification of iron and zinc on physical, nutrition, rheological and storage properties of wheat flour. J. Cereal Sci., 116, 103868. https://doi.org/10.1016/j.jcs.2024.103868

Ledari, S.A., Milani, J.M., Shahidi, S.A., Golkar, A. (2024). Comparative analysis of freeze drying and spray drying methods for encapsulation of chlorophyll with maltodextrin and whey protein isolate. Food Chem.: X, 21, 101156. https://doi.org/10.1016/j.fochx.2024.101156

Lekshmi, R.G.K., Tejpal, C.S., Anas, K.K., Chatterjee, N.S., Mathew, S., Ravishankar, C.N. (2021). Binary blend of maltodextrin and whey protein outperforms gum Arabic as superior wall material for squalene encapsulation. Food Hydrocolloids, 121, 106976. https://doi.org/10.1016/J.FOODHYD.2021.106976

Li, Y.O., González, V.P.D., Diosady, L.L. (2023). Microencapsulation of vitamins, minerals, and nutraceuticals for food applications. In: R. Sobel (ed.), Microencapsulation in the Food Industry. https://doi.org/10.1016/B978-0-12-821683-5.00027-3

Ohanenye, I.C., Emenike, C.U., Mensi, A., Medina-Godoy, S., Jin, J., Ahmed, T., …, Udenigwe, C.C. (2021). Food fortification technologies: Influence on iron, zinc and vitamin A bioavailability and potential implications on micronutrient deficiency in sub-Saharan Africa. Sci.

Afr., 11, e00667. https://doi.org/10.1016/J.SCIAF.2020.E00667

Olson, R., Gavin-Smith, B., Ferraboschi, C., Kraemer, K. (2021). Food fortification: The advantages, disadvantages and lessons from Sight and Life programs. Nutrients, 13(4), 1118. https://doi.org/10.3390/nu13041118

Ośko, J., Pierlejewska, W., Grembecka, M. (2023). Comparison of the potential relative bioaccessibility of zinc supplements – in vitro studies. Nutrients, 15(12), 2813. https://doi.org/10.3390/nu15122813

Poopan, B., Kasorn, A., Puttarat, N., Kasemwong, K., Pachekrepapol, U., Taweechotipatr, M. (2024). Freeze drying microencapsulation using whey protein, maltodextrin and corn powder improved survivability of probiotics during storage. Food Sci. Biotechnol., 34, 959–970. https://doi.org/10.1007/s10068-024-01706-w

Pratap-Singh, A., Leiva, A. (2021). Double fortified (iron and zinc) spray-dried microencapsulated premix for food fortification. LWT, 151, 112189. https://doi.org/10.1016/j.lwt.2021.112189

Qin, R., Pang, L., Hu, H., Jiang, Y., Lv, H., Ye, K., … Lin, Y. (2025). Associations of maternal dietary iron intake during pregnancy with infant neurodevelopment: evidence from a prospective cohort study. Nutr. J., 24(1), 131. https://doi.org/10.1186/s12937-025-01197-3

Qiu, L., Frazer, D.M., Hu, M., Song, R., Liu, X., Qin, X., …, Wang, X. (2025). Mechanism and regulation of iron absorption throughout the life cycle. J. Adv. Res., 77, 107–118. https://doi.org/10.1016/j.jare.2025.01.002

Shilpashree, B.G., Arora, S., Kapila, S., Sharma, V. (2020). Whey protein-iron or zinc complexation decreases prooxidant activity of iron and increases iron and zinc bioavailability. LWT, 126, 109287. https://doi.org/10.1016/j.lwt.2020.109287

Singh, P., Prasad, S. (2023). A review on iron, zinc and calcium biological significance and factors affecting their absorption and bioavailability. J. Food Compos. Anal., 123, 105529. https://doi.org/10.1016/j.jfca.2023.105529

Sirichokworrakit, S., Aukkanit, N., Sangsuwon, C. (2025). Optimizing encapsulation strategies for enhanced antioxidant stability of Wolffia globosa extracts: A comparative study of maltodextrin, gum arabic, and whey protein concentrate. Appl. Food Res., 5(1), 101030. https://doi.org/10.1016/J.AFRES.2025.101030

Subroto, E., Indiarto, R., Andoyo, R. (2023). Bioavailability of iron and its potential to improve the immune system and ward off COVID-19: a review. Food Res., 7(1), 76–92. https://doi.org/10.26656/fr.2017.7(1).701

Zhang, B., Wang, R.M., Chen, P., He, T.S., Bai, B. (2022). Study on zinc accumulation, bioavailability, physicochemical and structural characteristics of brown rice combined with germination and zinc fortification. Food Res. Int., 158, 111450. https://doi.org/10.1016/j.foodres.2022.111450